Analysis of the fixing process of FBG optical sensors for thermomechanical monitoring of aerospace applications

Analysis of the fixing process of FBG optical sensors for thermomechanical monitoring of aerospace applications

Alessandro Aimasso, Matteo D.L. Dalla Vedova, Alfredo Esposito, Paolo Maggiore

Department of Mechanical and Aerospace Engineering, Politecnico di Torino, Italy

alessandro.aimasso@polito.it matteo.dallavedova@polito.it

Abstract. In aerospace, lots of components can be defined as "safety critical". As a result, it is crucial to early identify the failure precursors when the effects on the systems performances are still practically insignificant. For this reason, complex networks of sensors had been developed and integrated into different parts to monitor several operational parameters, useful for evaluating their health (such as such as temperatures, displacements, vibrations, etc). Clearly, due to the importance of data collected, the technology employed shall be very reliable, even while working in harsh environments. Sensors based on optical fiber Bragg grating (FBG) meet these requirements. However, the fiber's integration process in the considered system is really crucial, from the moment that it could influence the sensors output. In this regard, gluing the optical sensors is really a critical activity, because the effects of the glue's retire and its viscous assessment shall be analysed and quantified. In this work, it was done by comparing performances of two equal samples, each one with an FBG glued on it. The first sample was prepared about two months before the second one. Furthermore, data from both FBG have been collected from the gluing phase of the second sample and in the following days. The results showed that the assessment of the resin evolved in different phases, but all of them were united by the fact that the overall process makes sensors measures not reliable during this specific transitory phase. By observing the evolution of the linear fit gradients, it can be stated that the variations reached their maximum in the middle of the gluing process, when the fiber was detached from the tensioning device. Finally, at the end of the overall process, data output resulted stable, so making FBG employable for reliable thermal or strain measures.

1. Introduction

Over the last few years optical fiber technology has found an increasing number of applications in the aerospace sector. Optical fiber transmission lines along with FBG (Fiber Bragg Grating) sensors offer multiple advantages compared to conventional ones. In traditional structural health monitoring systems, different types of sensors are used: strain gauges, piezoelectric sensors, ultrasonic sensors etc. These commonly employed sensors require an electrical transmission line to be connected to the monitoring system. This type of transmission line is the main downside of traditional monitoring system. Moreover, some of the main disadvantages are represented by a considerable amount of weight due to the materials used (i.e. copper wires), vulnerability to electromagnetic interference, relatively low bandwidth, low corrosion resistance and all the potential problems related to electrical wiring. Using optical fiber sensors (FBGs) allows the implementation of an optic fiber transmission line, thus solving some of the issues associated with electrical lines. Among the advantageous characteristics are the overall lightness, greater bandwidth, electromagnetic interference invulnerability, reduced signal dispersion and high resistance to harsh conditions and corrosion.

FBG sensors share the same characteristic as the optic fiber transmission line as they are embedded in the fiber itself. In addition, they are characterized by high sensitivity, multiplexing capabilities and electrically passive operation. The main purpose of this experimental study is to investigate the reliability of FBG sensor's mounting methods. The trials were carried out using composite material samples. Optical fibers containing FBG sensors were fixed on the samples. The fibers were attached using epoxy resin.

1.1. Generalities about optical fiber

Optical fiber is a thin transparent fiber in which light can be transmitted over long distances with minimal loss of signal. The most common material used in optical fiber production are silica or polymers. The optical fiber presents a cylindrical structure with several concentric layers: the core, the cladding, and the coating. The core is the most internal component, allowing the passage of the needed information in the form of a light signal. It is normally made of glass or a polymeric substance and has a maximum thickness of 50 μm. The cladding is the intermediate layer that is required to ensure the proper operation of the complete optical fiber. It has a diameter of 125 μm in general. The coating is the outer layer, and it is used to protect the structure from potential damage due to the fiber's extremely low bending resistance. Because of its high brittleness, several extra outer layers might be added to increase mechanical strength. The fundamental principle behind the operation of optical fibers is the total internal reflection. A laser beam traveling in the fiber, when hits the interface between the fiber and another medium with a lower refractive index at a sufficiently low angle, it is reflected and keeps traveling along the fiber. The critical angle, which is the minimum angle that the laser beam has to have to be internally reflected, can be calculated with Snell's law:

$$n_1 sen(\theta_1) = n_2 sen(\theta_2) \qquad (1)$$

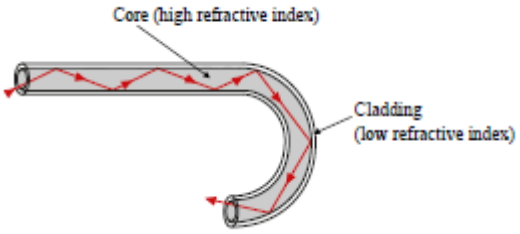

Figure 1. *Optical fiber structure*

2. Data acquisition system

The sensors employed in the tests are Fiber Bragg Gratings (FBG). Fiber Bragg gratings are a type of reflector embedded in the optical fiber. The reflector is created by periodically varying the refractive index of the material through photo inscription. When light hits the FBG a specific wavelength is reflected (i.e. Bragg wavelength), this wavelength satisfies the Bragg relation:

$$\lambda_B = 2n_{EFF}\Lambda_G \qquad (2)$$

where n is the effective refractive index of the core and Λ_G is the index modulation pitch (i.e. grating pitch). When manufacturing the FBG, the index grating can be varied to match the reflected wavelength to a specific one. This is fundamental when assembling an FBG based sensor system, multiple sensors can be multiplexed on a single fiber. The wavelengths that are not reflected by one of the FBGs can be reflected by a consecutive one, to do so all the different sensor must have a different Bragg wavelength. The main characteristic that makes FBGs good sensors is their responsiveness to external disturbances like changes in temperature and strain. These perturbations produce a variation in the refractive index of the material and in the grating pitch, consequently a shift in the reflected signal can be observed.

The relation between the shift of the signal and changes in strain and temperature is described by the following equation that links the variation of the Bragg's wavelength $\Delta\lambda_B$ to the applied strain ε and the variation in temperature ΔT [1]

$$\Delta\lambda_B = 2n\Lambda\left(\left\{1-\left(\frac{n^2}{2}\right)[P_{12}-\nu(P_{11}+P_{12})]\right\}\varepsilon+\left[\alpha+\frac{\left(\frac{dn}{dT}\right)}{n}\right]\Delta T\right) \qquad (3)$$

where P_{ij} are the piezo (Pockel's) coefficients of the stress-optic tensor, ν is Poisson's ratio and α is the coefficient of thermal expansion (CTE) of the fiber material. The equation (4) can be also written more generally as

$$\Delta\lambda_B = \lambda_B(K_\varepsilon\varepsilon + K_T\Delta T) \qquad (4)$$

The two main components of an FBG measuring system are the interrogator, that sends a laser beam into the FBGs, and the computer that processes the signal.

The operating principle of the interrogator is the following: through the connection it sends a light signal on a wide range of wavelengths into the fibers, when a BW (Bragg wavelength) is reflected it travels through the fiber to the interrogator where it is detected by the photodetectors, the light signal is then processed and sent as a digital signal to the computer. On the computer the signal is processed by SmartSoft. The interrogator used in this work is SmartScan by SmartFibre. It can read wavelengths from 1528 to 1568 nm, while working on four independent channels. For each channel, a maximum of 16 FBGs could be detected, with a frequency of acquisition of at most 25 kHz.

The software used during this work is SmartSoft: it elaborates the signal produced by the interrogator and allows to set the interrogator to match the experimental setup. The user can adjust various parameters that affect the acquisition rate of the SmartScan and the data processing rate of the software. Additional settings that can be adjusted are the number of channels and the number of FBGs per channel. The signals being received are shown in the lower half of the screen along with FBG peaks and their correspondent wavelength. Once the instrument is set up, the acquisition can begin. When starting an acquisition there are two options: a simple log or a scheduled log. A simple log is an acquisition that will last a specified amount of time. During that log time the reflected wavelengths will be registered at a set rate that depends on the chosen acquisition rate. The schedule log will automatically repeat the simple log acquisition at regular intervals in time until the acquisition is manually stopped.

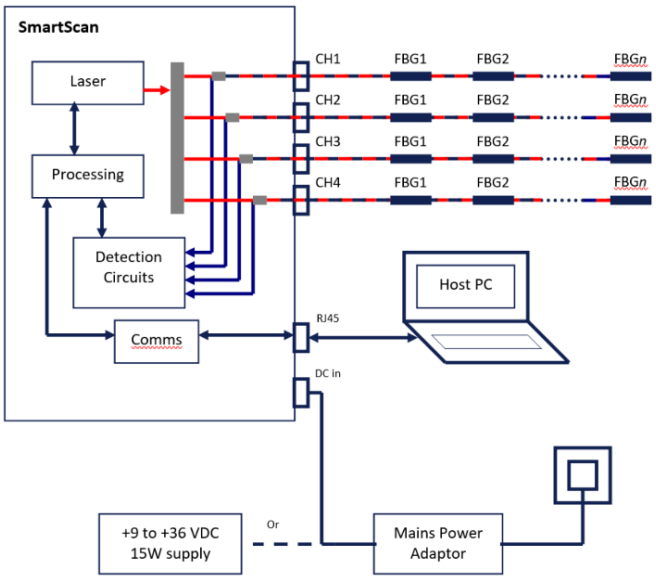

Figure 2. *Data Acquisition system*

3. Test campaign

The aim of the experiment was to study how the fiber tension was affected by the settlement of the resin. To do so, the variation in the tension of the fiber was observed by monitoring the changes in the reflected wavelength. As shown in the equation (4), these changes are linked to perturbations in strain and temperature of the fiber. As we are interested exclusively in tension changes, temperature variation introduces noise in the gathered data. For the hole length of data gathering the sample is positioned beside an older one (without strain variation due to settlement). The old and new samples have to be identical, same shape, same sensor (same BW) and sensor position, same method of fiber mounting and same preload. By placing the two samples close to each other, their temperature is the same throughout the data gathering. The aged sample is exclusively subjected to changes in temperature, while the newest is subjected to both changes in temperature and strain due to settlement. Considering the linear correlation between $\Delta\lambda$ and $\Delta\varepsilon$ and ΔT [1-3], the $\Delta\lambda_T$ in the newest sample is equivalent to the λ in the aged sample, the latter can be subtracted from the λ in the newest sample. Thus we are left with λ_ε of the newest sample:

Old sample:

$$\Delta\lambda_{os} = \Delta\lambda_{T,os}$$

New sample:

$$\Delta\lambda_{ns} = \Delta\lambda_{T,ns} + \Delta\lambda_{\varepsilon,ns}$$

As

$$\Delta\lambda_{T,os} = \Delta\lambda_{T,ns}$$

$$\Delta\lambda_{\varepsilon,ns} = \Delta\lambda_{ns} - \Delta\lambda_{T,ns} = \Delta\lambda_{ns} - \Delta\lambda_{os} \qquad (5)$$

3.1. Samples preparation

To obtain a precise tension in the fiber, the samples were mounted on an optical breadboard. The samples were fixed on two 3D printed supports with four bolts. The same bolts, used to fix the sample, secured the supports to the optical breadboard. The setup was completed by a linear translator attached to two scissor jacks. The translator was used to apply tension to the fiber, while the jacks were used to control the translator height and consequently ensure that the fiber was placed as close as possible to the surface of the sample. The first step of the fiber tensioning was gluing one side of the fiber to the sample, the other side was attached to a support that was later fixed to the translator. Once the acrylic glue was hardened, tension could be applied to the fiber. To control the tension, the fiber was connected to the interrogator. A tension on the fiber corresponded to a strain and consequently to a shift of the Bragg wavelength which was detected by the interrogator. The tension on the fiber was increased until a precise shift was reached. The desired shift was calculated using the relation (4).

The maximum strain that can be applied to the fiber is 10'000 με. Once the interrogator reads the expected wavelength λ_f , tensioning can be stopped and resin can be applied to the sample to lock the fiber in position. After the curing time is passed, the fiber can be removed from the tensioning device.

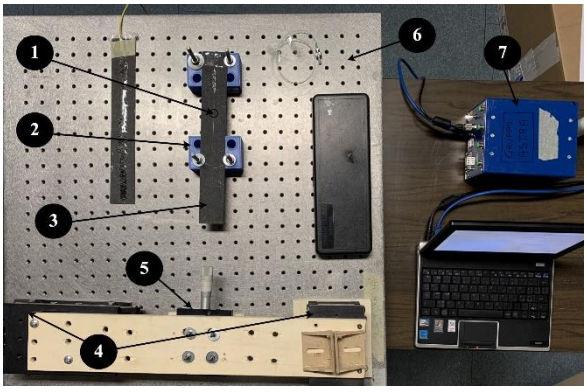

Figure 3. *Test bench organization*

Table 1. *Tools employed in the test bench*

1	Optical fiber
2	3D printed support
3	Sample
4	Scissor jack
5	Linear translator
6	Optical breadboard
7	Interrogator

The production process was the same for the two samples. The only dissimilarity between the two samples was the production date. A sensor was attached to the first sample 3 months prior to the sensor on the second sample. A preloaded generating strain of 1500 με was applied. The characteristics of the sample are resumed in table.

Table 2. *Samples characteristics*

Material	carbon-fibre/epoxy laminate (14 layers of unidirectional carbon-fibre)
Dimensions	260x350x1.6 mm
Sensors	1 FBG sensor with λ_b = 1540 nm

The sensors were mounted at mid-span of the samples. Despite the two sensors used had the same BW, at the time of sample production, the wavelengths were slightly different. For each sensor the final wavelength that had to be reached was calculated. Λ_0 is the measure reflected wavelength at rest. Value of λ_0 is the shift corresponding to a 1500 $\mu\varepsilon$" preload.

3.2. Data acquisition

Once the second fiber was tensioned and resin was applied to it, data gathering started. The aged and new samples were placed close to each other, this guaranteed their temperature to be identical during the hole process. Successively the fibers were connected to the interrogator. The fiber on the new sample was connected to channel 1 of the interrogator, the one on the old sample was connected to channel 2. Throughout the data collection, the samples were left in a room with no temperature control system. The acquisition rate was set at 25 Hz. The interrogator was then set to effectuate one acquisition per minute. The duration of the single acquisition was set to be 1 second. That setting resulted in 60 acquisitions (logs) per hour, each log consisting of 25 measurements, acquired at intervals of 40'000 microseconds. The log produced every minute was saved as a *.log* file. The data gathering lasted for 157.4 hours (6 days, 13 hours and 24 minutes). For the first days of the experiment, the resin was left to cure while the fiber was still attached to the tensioning device. The resin was periodically checked in order to assess its curing stage. After 3 days, when the curing was complete, the connection between the fiber and the tensioning device was cut off.

4. Results and discussion

Once the data collection ended, the resulting files were processed through a MATLAB script. Each log file contained two significant information: the start time of the log and 25 measurements. The mean value of the 25 measurements was calculated for each log file and associated to each start time. This a single value of λ was associated to each log, that is a single value of λ per minute. In figure 4 the raw data can be observed.

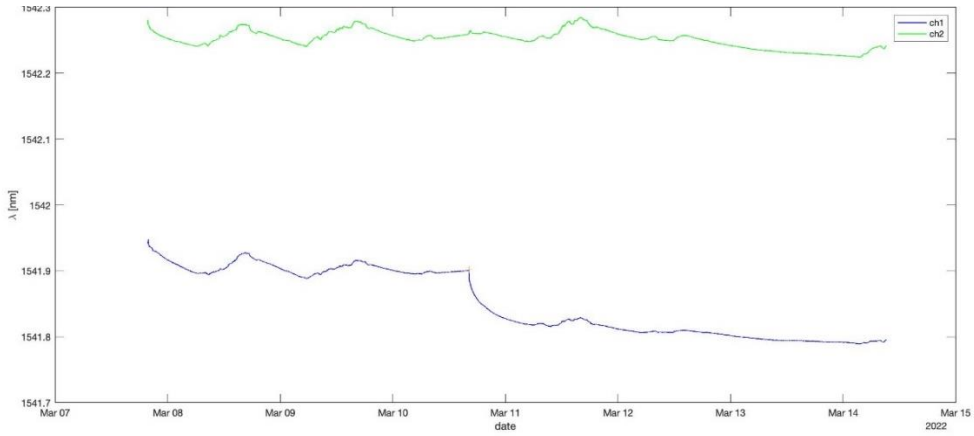

Figure 4. *Raw data*

To make the diagram easier to be read, data were normalized using the mean value of the overall acquisition period was employed:

$$\lambda_m = \frac{1}{N}\sum_{i=1}^{N} \lambda_i \quad (6)$$

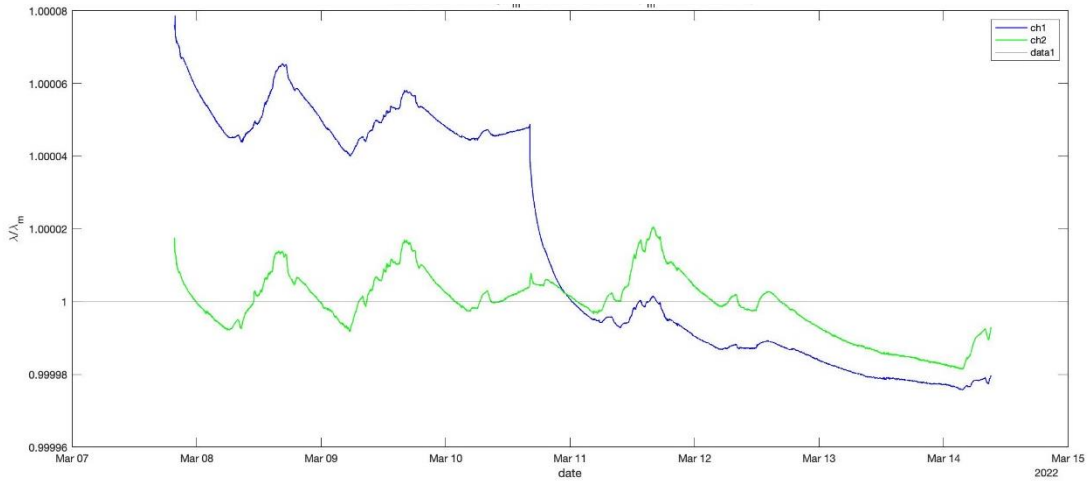

Figure 5 *Curing process: normalized data using λ_m as value of reference*

To partially eliminate the temperature fluctuation, normalized data can be processed using the moving average. In figure 6 the moving average is applied on a daily window to match the temperature fluctuation using the MATLAB function *movmean*. This function calculates for each moment in time a new value, λ_n, which is the mean value of neighbouring elements:

$$\lambda_n = \frac{1}{N}\sum_{i=N}^{n+N-1} \lambda_{i-\frac{N}{2}} \quad (7)$$

Where N=24*60=1440 as at each minute in time a λ is associated and the moving average has to be calculated over a sliding window of 24 hours.

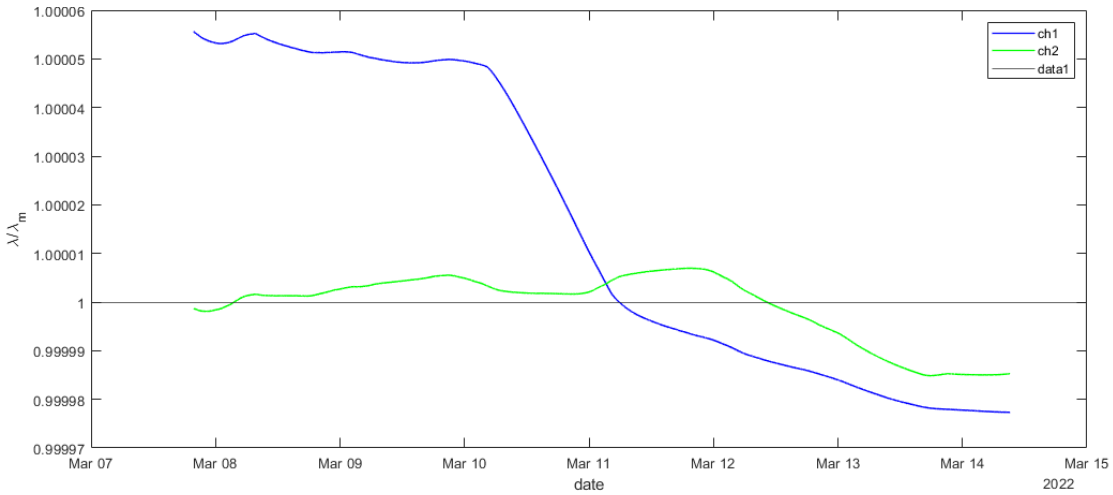

Figure 6. *Normalized data with moving average*

As stated in the previous chapter, the method chosen to eliminate the dependence of λ_B variation from temperature variation is subtracting the data of the aged sample from the data of the new sample. The subtracted data can be observed in figure 7. It can be observed from the diagram that the λ_B variation caused by the temperature cycling are not completely eliminated by using the previous method. Thus, as viewable in the picture, also the moving average is used on a daily window and it is calculated using equation (7).

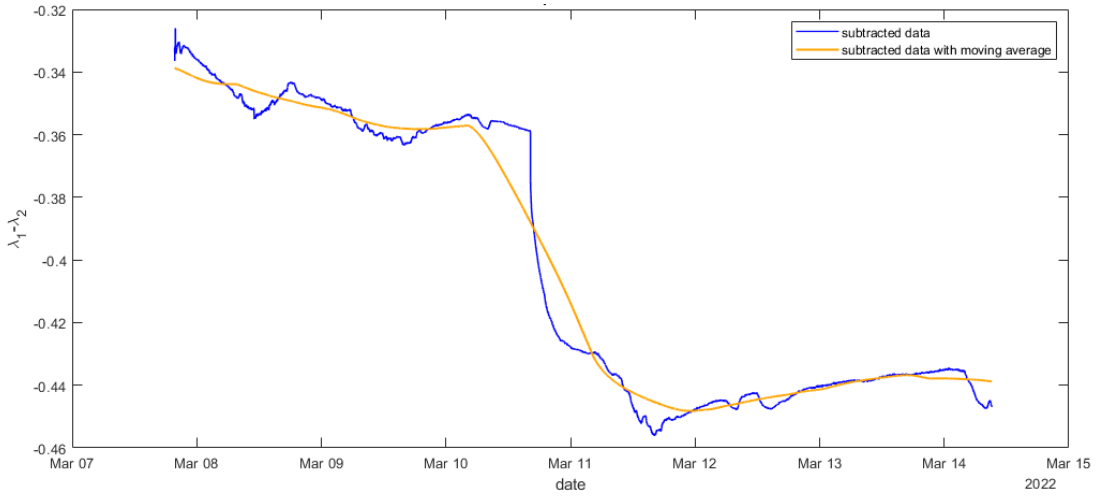

Figure 7. *Subtracted data and subtracted data with moving average*

From figure 7 three different sections in the data gathering process can be identified. The first part goes from the beginning of the experiment to the detaching of the fiber from the tensioning device, in this period the resin is curing. The second part can be identified as the section in which the settlement of the resin prevails over the temperature oscillations, in this period the decrease in strain is so rapid that temperature oscillations are not appreciable. The third part starts when temperature oscillations become visible again and lasts until the end of the data gathering process. This division is highlighted in figure 8. To compare the different sections, a linear fit was found for each one of them: in section I, the gradient is $-8.71*10^{-8}$, in section II is $-91.1*10^{-8}$ and in section III is $3.21*10^{-8}$. The linear fits can be seen as red lines always in figure 8 Finally, after 10 days a new data gathering was carried out for three days. Data showed as, once ended the resin curing process, the results became the same for both the samples.

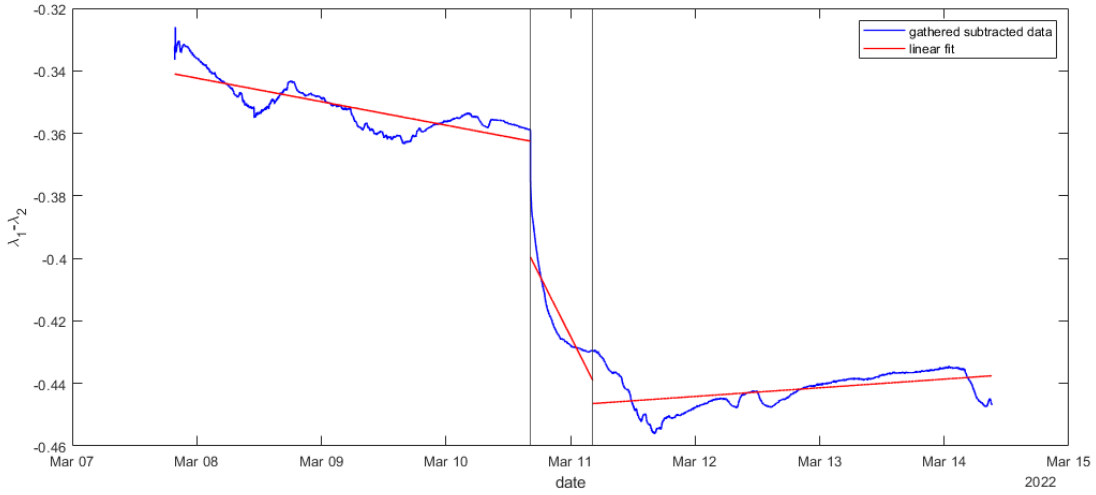

Figure 8. *Subtracted data and linear fit*

5. Conclusions

By observing the evolution of the linear fit gradients, it can be stated that the variations in λ reach their maximum when the fiber is detached from the tensioning device. In section II the gradient is more than 10 times higher than the one in section I and circa 30 times higher than the one in section III.
Shortly after detaching the sensors from the tensioning device, it is advisable not to use the sensors since the measurements would be influenced by the settlement of the fiber in the resin. The settlement lasted approximately 12 hours, to be on the safe side a waiting period of 24 hours can be advised.

Whilst the difference in the gradient between different phases of the experiment were great enough to notice the settlement of the fiber in the resin, temperature variations were not eliminated using the originally chosen method. In the second experiment it was found that for strains of a certain magnitude, such as the one the fibers were subjected to in the static tests, a difference in the fiber tension does not result in a difference in the measured λ. The same cannot be affirmed for strains of different magnitude (lower or greater) and for temperature variations. For this reason, the main cause in the partial failure of the used method can be supposed to reside in a difference between the tension of the fibers in the two samples, which resulted in different $\Delta\lambda_T$.

References

[1] Dalla Vedova, M.D.L., Berri, P.C., Aimasso, A., *Environmental sensitivity of Fiber Bragg Grating sensors for aerospace prognostics,* Proceedings of the 31st European Safety and Reliability Conference, ESREL 2021,2021, pp. 1561–1567

[2] Aimasso, A.,Dalla Vedova, M.D.L., Maggiore, P.,Quattrocchi, G.; Study of FBG-based optical sensors for thermal measurements in aerospace applications; Journal of Physics: Conference Series, 2022

[3] Aimasso, A., Vedova, M.D.L.D., Maggiore, P.; *Innovative sensor networks for massive distributed thermal measurements in space applications under different environmental testing conditions*; 2022 IEEE 9th International Workshop on Metrology for AeroSpace, MetroAeroSpace 2022 - Proceedings, 2022, pp. 503–508

[4] Alan D. Kersey, Michael A. Davis, Heather J. Patrick, Michel LeBlanc, and K. P. Koo; "*Fiber Grating Sensors*"; Journal Of Lightwave Technology (1997)

[5] Iain McKenzie A, Ibrahim S, Haddad E, Abad S, Hurni A and Cheng L; *Fiber Optic Sensing in Spacecraft Engineering: An Historical Perspective From the European Space Agency*; Frontiers in Physics, 2021